Familial aortic aneurysm in Leonberg dogs

Valérie Chetboul, DVM, PhD; Dominique Tessier, DVM; Nicolas Borenstein, DVM, PhD; Françoise Delisle, DVM; Luca Zilberstein, DVM; Guillaume Payen, DVM; Eric Leglaive, DVM; Brigitte Franc, DM, PhD; Geneviève Derumeaux, DM, PhD; Jean-Louis Pouchelon, DVM, PhD

- Spontaneous aortic aneurysm is a rare condition in the dog.
- The diagnosis of aortic aneurysm is aided by the use of complementary imaging techniques such as transthoracic and transesophageal echocardiography and magnetic resonance imaging.

A 6-month-old male Leonberg dog was referred because of signs of severe depression. The dog was from a litter of 12, 3 of which died shortly after birth. On physical examination, the dog was lethargic and small for its age (18 kg [39.6 lb]). Rectal temperature (38.6°C [101.5°F]), hydration, capillary refill time, and color of the mucous membranes were within reference limits. The conformation of the dog appeared slightly disproportionate, with short limbs and a flat face. Generalized slight hypermobility of the joints was observed. The thorax was also deformed. The ventrodorsal dimension of the thorax was decreased, and palpation revealed discrete internal bulging of certain ribs. Maximum cardiac impulse was more prominent on the right side of the thorax. Femoral arterial pulses were decreased bilaterally; however, cardiac auscultation revealed no abnormalities. Radiographs of the thorax were obtained. Radiography revealed marked dilatation of the aorta without substantial cardiomegaly.

Arterial blood pressure was measured indirectly on fore- and hind limbs by use of the oscillometric method[a] with a neonatal cuff (6 to 11 cm). Five measurements were performed on each limb. Mean systolic and diastolic blood pressures were 120 and 95 mm Hg, respectively, for forelimbs, and 105 and 90 mm Hg for hind limbs (reference range for systolic blood pressure, 100 to 160 mm Hg; reference range for diastolic blood pressure, 60 to 100 mm Hg).[1] Systemic hypertension was, therefore, excluded.

Electrocardiography revealed a heart rate of 100 beats/min and a regular sinus rhythm. **Transthoracic echocardiography (TTE)** was performed with a 3.5- to 5-MHz transducer[b] and revealed marked dilatation of the aorta. The aneurysm extended from the aortic root to the aortic arch **(Fig 1)**. Despite the marked increase in size of the aortic root and ascending aorta (46 mm; reference range, 27.3 to 29.3 mm),[2] the aortic valves and diameters of the left atrium (26 mm; reference range, 25.7 to 28.3 mm) and left ventricle (diastolic diameter of left ventricle, 44 mm; reference range, 43.6 to 47.8 mm; systolic diameter of left ventricle, 29 mm; reference range, 27.2 to 30.2 mm)[2] were normal with a shortening fraction of 33%. An aortic flow profile obtained from the left apical 5-chamber view was also normal (maximal systolic velocity, 1.2 m/s; reference range, 0.83 to 1.53 m/s).[3] Color flow Doppler echocardiography revealed minor aortic insufficiency with a plateau-shaped profile on the continuous-wave spectral Doppler. Different views identified several channels along the aortic wall from the sinus of Valsalva to the aortic arch. Color flow Doppler echocardiography detected blood flow in the lumen of these channels. Mild dilatation of the pulmonary artery was also observed. However, flow through the pulmonary and tricuspid valves and the morphology of the right side of the heart were normal. Small hypoechoic and anechoic structures were observed in the pericardial space posterior to the left ventricle.

Anesthesia was induced with etomidate[c] (0.5 mg/kg [0.23 mg/lb], IV) and maintained with isoflurane (1 to 2%). **Transesophageal echocardiography (TEE)** was performed during general anesthesia with a 5-MHz transducer with M-mode, 2-dimensional, and Doppler capabilities.[d] Smoke-like echos were observed in the dilatation of the ascending aorta that suggested blood stasis. Aortic

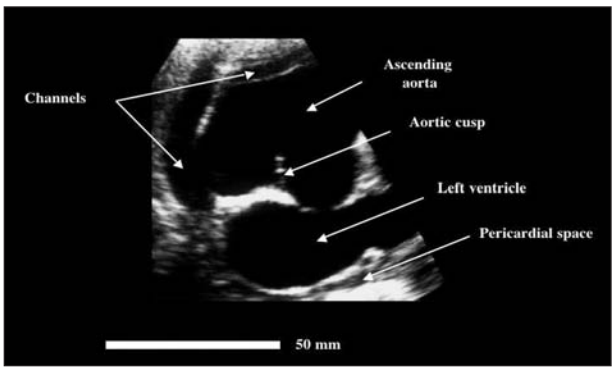

Figure 1—Transthoracic echocardiographic, right parasternal long-axis view of the ascending aorta in a dog. Notice that the diameter of the ascending aorta is markedly increased and larger than that of the left ventricle. Two anechoic channels are along the aortic wall. The pericardial space contains anechoic and hypoechoic structures.

From Unité de Cardiologie d'Alfort (Chetboul, Tessier, Pouchelon), Centre de Cancérologie Vétérinaire (Delisle), Service de Chirurgie (Zilberstein), and Unité Pédagogique de Médecine (Payen), Ecole Nationale Vétérinaire d'Alfort, 94704 Maisons-Alfort Cedex, France; the Institut Mutaliste Montsouris, Centre d'Expérimentation et de Recherche Appliquée de la Fondation de l'Avenir, 75014 Paris, France (Borenstein); the Clinique vétérinaire, 19 avenue de Royaumont, 95270 Viarmes, France (Leglaive); the Service d'anatomie et cytologie pathologique, Hôpital Ambroise Paré, 9 avenue Charles de Gaulle, 92100 Boulogne Billancourt, France (Franc); and the Service de Cardiologie et INSERM E 9920, Centre Hospitalier Universitaire Charles Nicolle, 1 rue de Germont, 76031 Rouen, France (Derumeaux).

Presented at the 27th World Small Animal Veterinary Association Congress, Grenada, Spain, October 2002.

The authors thank Drs. Laborde, Behr, Crespeau, Fontaine, Devauchelle, and Dandrieux for technical assistance.

Address correspondence to Dr. Chetboul.

stenosis was not detected, but the minor aortic insufficiency identified via TTE was well observed. Several TEE views confirmed that the channels observed along the aorta were not caused by aortic dissection but created by plication and twisting of the ascending aorta (**Fig 2**).

Magnetic resonance imaging (MRI)[e] of the heart was performed during general anesthesia. Anesthesia was induced with propofol[f] (5 mg/kg, IV) and maintained with isoflurane (1 to 2%). Gadolinium chelate[g] (0.4 mL/kg [0.18 mL/lb], IV) was administered, and spatial 3-dimensional maps were obtained. Magnetic resonance imaging excluded aortic dissection and aortic coarctation and confirmed a marked dilatation of the aorta (49 mm, nearly 2 times the normal diameter). The aortic dilatation was symmetric and involved the full circumference of the aortic wall. This important arterial abnormality, also called fusiform aortic aneurysm, extended from the ascending aorta to the first few centimeters of the descending aorta (**Fig 3**). Dilatation of all principal thoracic arteries (pulmonary trunk, brachiocephalic trunk, and left subclavian artery) was also identified. The left subclavian artery had an unusual curved course.

Because thoracic aortic aneurysms are frequently associated with abdominal aneurysms in human patients, ultrasonography of the abdomen was performed.[4] No abnormalities were detected.

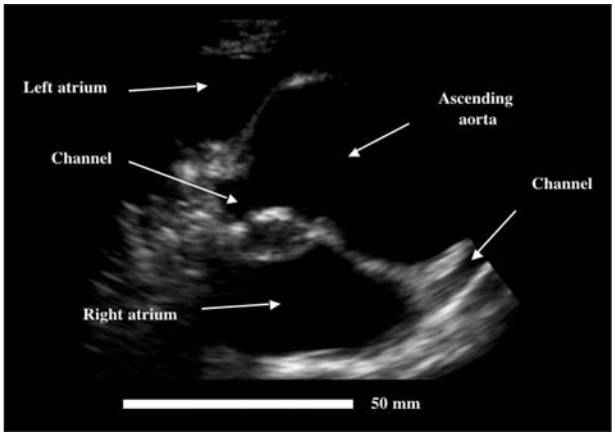

Figure 2—Transesophageal echocardiographic image of the ascending aorta of the dog in Figure 1. Notice the channels along the aorta created by plication and twisting of the ascending aorta.

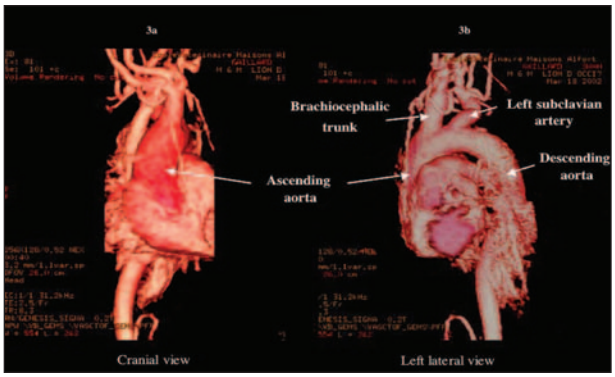

Figure 3—Cranial (A) and left lateral (B) magnetic resonance images of the heart of the dog in Figure 1 after injection of gadolinium chelate. Notice marked dilatation of the ascending aorta. The aneurysm is fusiform and extends from the ascending aorta to the first few centimeters of the descending aorta. The left subclavian artery is curved.

The owner of the dog chose euthanasia. Dilatation of the thoracic aorta was confirmed at necropsy. The aorta was twisted and wrinkled from the aortic root to the aortic arch (**Fig 4**). Dilatation of the other thoracic arteries and the abnormal course of the left subclavian artery were also confirmed. The pericardium was opened, and cardiac lymphangectasia was identified, which explained the abnormal echoes in the pericardial space that were observed via TTE. The 4 cardiac chambers and the aortic cusps were normal.

Histologic examination revealed that the inner half of the media of the aorta, particularly at the level of the sinus of Valsalva, was focally destroyed and replaced by small round areas of acid mucopolysaccharide accumulation (**Fig 5**). Intramural hemorrhage and inflammato-

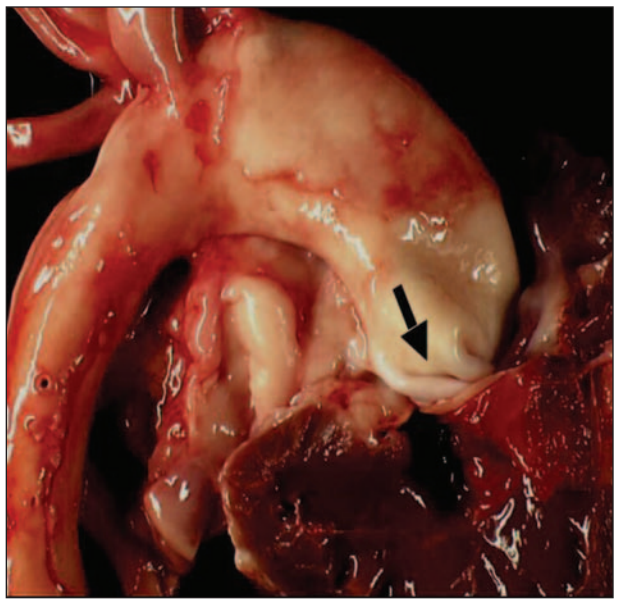

Figure 4—Photograph of a section of the ascending aorta of the dog in Figure 1. Notice that the root of the aorta (arrow) is plicated and twisted.

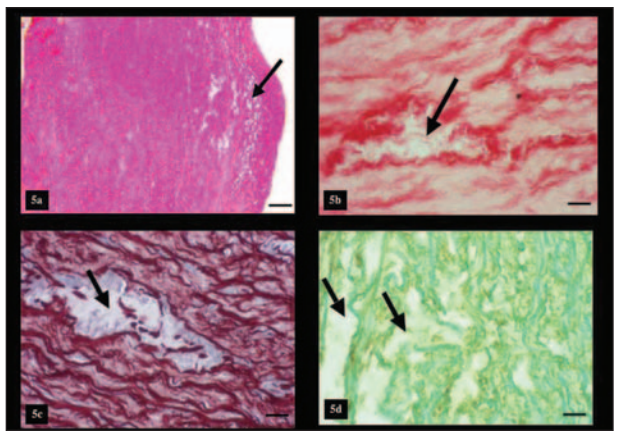

Figure 5—Photomicrographs of a section of the ascending aorta from the dog in Figure 1. A—The inner half of the media is focally destroyed and replaced by small round areas (arrow) of acid mucopolysaccharide. H&E stain; bar = 250 µm. B—The collagen fibers are thicker than in the rest of the media and disorganized. Notice a cystic area (arrow) between the collagen fibers. Sirius red-picric acid stain; bar = 25 µm. C—Fragmentation of the elastic fibers is associated with cystic areas (arrow). Orcein stain; bar = 25 µm. D—Microfibrils within the elastic fibers are disrupted by pseudocystic spaces (arrows). Immunohistochemical stain; bar = 50 µm.

ry cells were absent. Sirius red-picric acid stain was used to distinguish the collagen fiber network, which appeared disorganized. The elastic network (orcein stain) was preserved, except that a large amount of fragmentation and round areas that corresponded to multiple ruptures were observed. Immunoperoxidase techniques were performed on acetone-fixed frozen tissue sections by use of mouse monoclonal antibodies[h] against the muscle glycoprotein, fibrillin-1, a key structural component of microfibrils. Disrupted microfibrils around and inside pseudocystic spaces were observed.

A familial survey that included physical examination and TTE was performed on the 8 littermates and the dam and sire of the dog of this report. Measurements of the diameter of the aorta and left atrium were obtained by 2-dimensional TTE, with a short-axis right-sided parasternal view of the aortic valve in which commissures of the aortic valve cusps can be observed during diastole. The internal short-axis diameter of the aorta was measured along the commissure between the noncoronary and left coronary aortic valve cusps. The left atrium was measured by use of the same frame in a line that extended from and parallel to the commissure between the noncoronary and left coronary aortic valve cusps. Results of measurements obtained from all females (the dam and 4 littermates) and 2 male littermates were within reference ranges (left atrium-to-aorta ratio of 0.98 ± 0.17; range, 0.83 to 1.13).[5] However, 1 male littermate had a recurrent diaphragmatic hernia with 4 unsuccessful surgical repairs. In addition, the sire and 1 other male puppy had an abnormal dilatation of the ascending aorta (internal short-axis diameter, 52 and 41 mm, respectively; left atrium to aorta ratio of 0.54 and 0.53, respectively).[5] Moreover, similar to the dog in this report, several channels were observed along the aortic wall of the other male littermate, which suggested a similar twisted course of the aortic root and a marked delay in growth associated with generalized joint hypermobility.

The major cause of aortic dilatation in dogs is congenital aortic stenosis, which causes poststenotic dilatation of the ascending aorta.[6] The aortic dilatation observed in the dog in this report extended to the descending thoracic aorta. A diagnosis of aortic stenosis was excluded by use of color flow and spectral Doppler echocardiography. Because systemic arterial hypertension was also not detected, aortic aneurysm caused by coarctation or abnormal composition of the aortic wall was suspected.

Transesophageal echocardiography and MRI were performed, because these 2 techniques are known to be sensitive in the diagnosis of thoracic aortic malformations, especially aortic dissection and coarctation.[7-9] Use of TEE provided a precise analysis of the ascending aorta, whereas MRI enabled global exploration of the principal thoracic arterial trunks. Channels along the aortic wall were observed more clearly with TEE than TTE. Therefore, aortic dissection was excluded, and twisting of the ascending aorta was confirmed. Magnetic resonance imaging with gadolinium chelate was used to complement information obtained from these 2 echocardiography techniques. Gadolinium is a paramagnetic molecule with unpaired electrons that reduces the relaxation times of resonating nuclei and improves demarcation of vascular structures.[10] Gadolinium-enhanced MR angiography confirmed marked dilatation of the principal thoracic arterial trunks and a marked fusiform aneurysm of the aorta. Use of MRI also helped to exclude a diagnosis of aortic dissection and increased the certainty of the diagnosis obtained with TEE. One of the major advantages gained by the use of MRI was the definitive exclusion of aortic coarctation.

Spontaneous aortic aneurysm is well known in humans but uncommon in domestic animals. In humans, aortic aneurysm is often a component of an acquired process such as atherosclerosis or aortitis.[11] Aortic aneurysm may also be associated with congenital diseases (bicuspid aortic valve or coarctation of the aorta) and heritable disorders of connective tissue.[12,13] Aortic aneurysm has been reported in association with patent ductus arteriosus,[14] aortic coarctation,[15] *Spirocerca lupi* infection,[16] and degenerative processes[17,18] in dogs and systemic hypertension in cats.[19] In the dog of this report, a degenerative lesion of the aortic wall, similar to that found in human cystic medial necrosis, was confirmed.

Complications of aortic aneurysms include structural weakness of the aorta that may lead to fatal rupture of the arterial wall or medial aortic dissection,[20] which was not observed in the dog of this report. An aortic dilatation may also exert traction on the aortic valvular annulus and pull it apart. Aortic regurgitation may develop secondarily, as in the dog of this report.

The twist of the aorta, which appeared wrinkled, was an uncommon finding associated with aortic aneurysm. To our knowledge, it has never been described in dogs. The cause of this abnormality may be aortic dilatation and the weakened abnormal aortic wall. The decreased systolic and differential arterial pressures may also be attributed to the abnormal composition of the aortic wall.

All of the histologic lesions identified in the dog in this report were similar to those observed in cystic medial degeneration (cystic medial necrosis) in humans.[21] However, whether the disorganization of collagen and the disruption of fibrillin-1 and elastic fibers were primary or secondary features was unknown. Cystic medial necrosis of the aorta is well described in humans.[22] This arterial lesion is extremely rare in dogs. To our knowledge, it has been described in only 2 reports.[17,18] This abnormal degenerative condition is known to induce weakening of the aortic wall, which may, as in the dog of this report, progressively lead to an aneurysm.[23-26] In humans, cystic medial necrosis may be idiopathic or result from different familial connective tissue disorders, especially Marfan's syndrome and Ehlers-Danlos type IV syndrome, which are related to mutations of the fibrillin gene and the type III collagen gene, respectively.[12,27] These familial diseases may affect several arterial trunks. In severe Marfan's syndrome, skeletal and ocular anomalies are associated with cardiovascular problems.[28] No ocular lesions were observed in the dog of this report; however, as described in humans with Marfan's syndrome, a generalized joint hypermobility caused by laxity of the

supporting ligaments was detected in this dog and another male littermate. Moreover, 1 other male littermate had a recurrent diaphragmatic hernia. Recurrent hernias are well described in human connective tissue disorders such as Marfan's syndrome and Ehlers-Danlos syndrome,[12] which makes these 2 differential diagnoses more likely. In humans, the diagnosis may be obtained by use of cultured skin fibroblasts, which detects abnormalities of fibrillin or collagen production.[29] This diagnostic test was not used in any of the dogs of this report; therefore, the cause of the degenerative changes of the aorta remained unknown.

[a]Dinamap, Critikon Inc, Tampa, Fla.
[b]AU3 partner, Esaote Biosound, Indianapolis, Ind.
[c]Hypnomidate, Janssen-Cilag Inc, Titusville, NJ.
[d]Vingmed, System 5, GE Medical Systems, Milwaukee, Wis.
[e]Sigma Profile 0.5 tesla, GE Medical Systems, Milwaukee, Wis.
[f]Rapinovet, Schering-Plough Corp, Kenilworth, NJ.
[g]Dotarem, Guerbet LLC, Bloomington, Ind.
[h]Fibrillin-1 Ab-2 (clone 12A5-18), Neomarkers, Labvision Corp, Westinghouse, Calif.

References

1. Haskins SC. Monitoring the anesthetized patient. In: Thurmon JC, Tranquilli WJ, Benson GJ, eds. *Veterinary anesthesia.* 3rd ed. Baltimore: The Williams & Wilkins Co, 1996;409–424.

2. Boon JA. *Handy reference veterinary echocardiography: two dimensional and M-mode imaging* (laminated card). 1st ed. Jackson, Wyo: Teton NewMedia, 2001.

3. Gaber C. Doppler echocardiography. *Vet Clin North Am Small Anim Pract* 1991;3:500–519.

4. Isselbacher EM, Eagle KA, Desanctis RW. Diseases of the aorta. In: Braunwald E, ed *Heart disease: a textbook of cardiovascular medicine.* 5th ed. Philadelphia: WB Saunders Co, 1997;1546–1581.

5. Boon J, Wingfield W, Miller C. Echocardiographic indices in the normal dog. *Vet Radiol* 1983;24:214–221.

6. Kittleson MD, Keene RD. Radiography of the cardiovascular system. In: Kittleson MD, Keene RD. *Small animal cardiovascular medicine.* St Louis: CV Mosby Co, 1998;47–71.

7. Laissy J-P, Blanc F, Soyer P, et al. Thoracic aortic dissection: diagnosis with transesophageal echocardiography vs MR imaging. *Radiology* 1995;194:331–336.

8. Willens HJ, Kessler KM. Transesophageal echocardiography in the diagnostics of diseases of the thoracic aorta: part 1. Aortic dissection, aortic intramural hematoma, and penetrating atherosclerotic ulcer of the aorta. *Chest* 1999;116:1772–1779.

9. Nienaber CA, Spielmann RP, Von Kodolitsch Y, et al. Diagnosis of thoracic aortic dissection: magnetic resonance imaging vs transesophageal echocardiography. *Circulation* 1992;85:434–447.

10. Krinsky G, Reuss PM. MR angiography of the thoracic aorta. *Magn Reson Imaging Clin N Am* 1998;6:293–320.

11. Lindsay J. Diagnosis and treatment of diseases of the aorta. In: Fuster V, Alexander RW, O'Rourke RA, eds. *Hurst's the heart.* 10th ed. New York: McGraw-Hill Health Professions Division, 2001; 2375–2395.

12. Roman MJ, Devereux RB. Heritable aortic disease. In: Lindsay J Jr, ed. *Diseases of the aorta.* Philadelphia: Lea & Febiger, 1994;5–74.

13. Anderson PA. The molecular genetics of cardiovascular disease. *Curr Opin Cardiol* 1995;10:33–43.

14. Olsen D, Harkin KR, Banwell MN, et al. Postoperative rupture of an aortic aneurysmal dilatation associated with a patent ductus arteriosus in a dog. *Vet Surg* 2002;31:259–265.

15. Herrtage ME, Gorman NT, Jeffries AR. Coarctation of the aorta in a dog. *Vet Radiol Ultrasound* 1992;33:501–509.

16. Hamir AN. Perforation of the thoracic aorta in a dog associated with *Spirocerca lupi* infection. *Aust Vet J* 1984;61:64.

17. Bevilacqua G, Camici P, L'abbate A. Spontaneous dissecting aneurysm of the aorta in a dog. *Vet Pathol* 1981;18:273–275.

18. Colombo S. Arteriopatosi mucoide-cistica medioartica nel cane. *Clin Vet* 1958;81:65–72.

19. Wey AC, Atkins CE. Aortic dissection and congestive heart failure associated with systemic hypertension in a cat. *J Vet Intern Med* 2000;14:208–213.

20. Pretre R, Vonsesser LK. Aortic dissection. *Lancet* 1997;349: 1462–1464.

21. Nakashima Y, Kurozumi T, Sueishi K, et al. Dissecting aneurysm: a clinicopathologic and histopathologic study of 111 autopsied cases. *Hum Pathol* 1990;21:291–296.

22. Isner JM, Donaldson RF, Fulton D, et al. Cystic medial necrosis in coarctation of the aorta. *Circulation* 1987;75:689–695.

23. Fann JI, Miller DC. Descending thoracic aortic aneurysms. In: Baue AE, Gehe SS, Hammond GL, et al, eds. *Glenn's thoracic and cardiovascular surgery.* Stamford, Conn: Appleton & Lange, 1996: 2255–2272.

24. Zierler RE, Strandness DE. Hemodynamics for the cardiovascular surgeon. In: Moore WS, ed. *Vascular surgery: a comprehensive review.* Philadelphia: WB Saunders Co, 1993;179–204.

25. Fourtrakis GN, Yonas H, Sclabassi RJ. Saccular aneurysm formation in curved and bifurcation arteries. *Am J Neuroradiol* 1999; 20:1309–1317.

26. Howe LM, Boothe HW. Nitric oxide: a review for veterinary surgeons. *Vet Surg* 2001;30:44–57.

27. Dobrin PB, Mrkvicka R. Failure of elastin or collagen as possible critical connective tissue alterations underlying aneurysmal dilatation. *Cardiovasc Surg* 1994;2:484–488.

28. De Paepe A, Devereux R, Dietz H, et al. Revised diagnostic criteria for the Marfan syndrome. *Am J Hum Genet* 1996;62:417–426.

29. Minor RR, Sippola-Thiele M, McKeon J, et al. Defects in the processing of procollagen to collagen are demonstrable in cultured fibroblasts from patients with the Ehlers-Danlos and osteogenesis imperfecta syndromes. *J Biol Chem* 1986;261:10006–10014.